TITLE:

In Situ Vascularization of Injectable Fibrin/Poly(Ethylene Glycol) Hydrogels by Human Amniotic Fluid-Derived Stem Cells

AUTHORS:

Omar M. Benavides[1], Abigail R. Brooks[1], Stephanie Cho[1], Jennifer Petsche Connell[1], Rodrigo Ruano[2,3], & Jeffrey G. Jacot[1,4]

AFFILIATIONS:

[1] Department of Bioengineering, Rice University, Houston, TX

[2] Fetal Center, Pavilion for Women, Texas Children's Hospital, Houston, TX

[3] Department of Obstetrics and Gynecology, Baylor College of Medicine, Houston, TX

[4] Congenital Heart Surgery Services, Texas Children's Hospital, Houston, TX

KEYWORDS:

Amniotic fluid-derived stem cells, Vasculogenesis, Hydrogels, Fibrin, Angiogenesis

CORRESPONDING AUTHOR:

Jeffrey G. Jacot

jeff.jacot@rice.edu

713-348-4446

6500 Main St. – MS 142

Houston, TX 77005

ABSTRACT

One of the greatest challenges in regenerative medicine is generating clinically-relevant engineered tissues with functional blood vessels. Vascularization is a key hurdle faced in designing tissue constructs larger than the *in vivo* limit of oxygen diffusion. In this study, we utilized fibrin-based hydrogels as a foundation for vascular formation, poly(ethylene glycol) (PEG) to modify fibrinogen and increase scaffold longevity, and human amniotic fluid-derived stem cells (AFSC) as a source of vascular cell types (AFSC-EC). AFSC hold great potential for use in regenerative medicine strategies, especially those involving autologus congenital applications, and we have shown previously that AFSC-seeded fibrin-PEG hydrogels have the potential to form three-dimensional vascular-like networks *in vitro*. We hypothesized that subcutaneously injecting these hydrogels in immunodeficient mice would both induce a fibrin-driven angiogenic host response and promote *in situ* AFSC-derived neovascularization. Two weeks post-injection, the average maximum invasion distance of host murine cells into the subcutaneous fibrin/PEG scaffold was 147±90μm after one week and 395±138μm after two weeks, the average number of cell-lined lumen per mm^2 was significantly higher in hydrogels seeded with stem cells (MSC, 36.5±11.4; AFSC, 47.0±18.9; AFSC/AFSC-EC, 32.8±11.6; MSC/HUVEC, 43.1±25.1) versus endothelial cells alone (AFSC-EC, 9.7±6.1; HUVEC, 14.2±8.8); a subset of these lumen were characterized by the presence of red blood cells. Select areas of cell-seeded hydrogels contained CD31-positive lumen surrounded by αSMA-positive cells, whereas control hydrogels with no cells only showed infiltration of αSMA-positive host cells. These results demonstrate the potential of cell from amniotic fluid to enhance vascularization of injectable fibrin/PEG hydrogels.

1. INTRODUCTION

One of the greatest challenges in regenerative medicine is generating clinically-relevant engineered tissues thicker than a few millimeters. The inability to provide functional vascularization is a key hurdle faced in designing tissue constructs larger than the *in vivo* limit of oxygen, nutrient, and waste diffusion, which is approximately 200 microns.[1-3] The lack of a rapidly developed vascular network in tissues beyond this limit will result in inadequate *in vivo* perfusion, increased hypoxia, and decreased cellular viability.[4-6]

Methods of ensuring perfusion in engineered tissues range from stimulating angiogenesis through the introduction of growth factors or biological materials that promote invasion of endogenous host capillaries,[7-9] to pre-forming vascular networks within scaffolds *in vitro* prior to implantation.[10-12]

Relying solely on spontaneous or chemotaxis-driven angiogenesis, which vary from tenths of a micron per day to several microns per hour,[13, 14] is generally not sufficient to achieve rapid and complete vascularization of thick constructs.[3, 7, 8] Alternatively, prevascularizing engineered tissues with exogenous cells provides well-formed vascular-like networks prior to implantation.[10, 12, 15] While some studies have shown that seeding endothelial cells into tissue constructs before implantation may improve *in vivo* perfusion and cell viability,[1, 16, 17] others have shown no difference between the rate of *in vivo* blood vessel formation in hydrogels pre-vascularized with endothelial cells *in vitro* compared to mesenchymal stem cell (MSC)-seeded hydrogels relying on *in situ* vascularization alone.[18] Studies have also shown that combining both endothelial cells and a perivascular cell source, such as MSCs or fibroblasts, is essential in the generation of robust functional vascular networks *in vivo*.[19-21]

One potential source of both endothelial and perivascular cell types is amniotic fluid-derived stem cells (AFSC).[22-24] Previous results from our lab suggest that AFSC in three-dimensional co-cultures act as a perivascular support cell source similar to MSC and that AFSC-derived endothelial cells (AFSC-EC) promote vascular network formation similar to mature endothelial cell.[25] Significant advantages to using AFSC in regenerative medicine strategies include broad differentiation capacity, rapid proliferation, and the potential for use in autologous therapies in neonates, such as an engineered cardiovascular patch for repair of congenital heart defects.[26, 27]

In addition to a source of vascular cell types, a suitable scaffold for the development of vascularization is critical.[28] Our laboratory has shown previously that fibrin/poly(ethylene glycol) (PEG) hydrogels provide a platform for cell encapsulation that promotes biocompatibility, mechanical stability, and vasculogenesis.[25] Fibrin is a versatile biopolymer that has a critical role in blood clotting, cellular-matrix interactions, wound healing, and angiogenesis,[29-31] and is widely used as a biomaterial for engineered adipose, dermal, and cardiovascular tissues.[32-34] Like most other natural materials though, the main disadvantages of using fibrin as a scaffold are low mechanical stiffness and rapid degradation,[35, 36] both of which can be mitigated by incorporation of PEG, an FDA-approved polymer with a wide range of medical and industrial applications.[25, 37, 38]

Based on this data, we hypothesized that subcutaneously injecting AFSC-seeded fibrin/PEG hydrogels in immunodeficient mice would both induce a fibrin-driven angiogenic response and promote AFSC-derived neovascularization. In this study, we evaluated the potential for *in situ* formation of clinically relevant vasculature by assessing the rate of host cell

invasion, the degree of cell-lined lumen formation, and the co-localization of vascular cell types within AFSC-seeded fibrin/PEG hydrogels.

2. MATERIALS AND METHODS

2.1. Isolation of Human AFSC

Primary human amniotic fluid (AF) was obtained from patients in their second trimester undergoing planned amnioreduction as part of a therapeutic treatment for twin-twin transfusion syndrome (TTTS) as previously described.[22, 39] The experimental protocol and informed consent forms were approved by the Institutional Review Boards of Baylor College of Medicine and Rice University.

Briefly, AF was centrifuged and collected cells were resuspended in modified α-Minimum Essential Media: 63% αMEM (Invitrogen, Carlsbad, CA), 18% Chang Basal Medium (Irvine Scientific, Santa Ana, CA), 2% Chang C supplement (Irvine Scientific), 15% fetal bovine serum (PAA Laboratories, Dartmouth, MA), and GlutaMAX (Invitrogen) at 37°C and 5% CO_2 in a humidified environment. Cells were passaged at 60-70% confluency, and AFSC were isolated through fluorescence-activated cell sorting for expression of the membrane receptor CD117/c-kit (1:100 antibody concentration, BD Biosciences, Bedford, MA; Dako-Cytomation MoFlo sterile cell sorter).

2.2. Endothelial Differentiation of AFSC

AFSC were differentiated into endothelial-like cells as previously described.[22] Briefly, c-kit$^+$ AFSC at passage 4 were plated at 3000 cells/cm^2 on gelatin-coated plates, allowed to attach for 24 hours in modified αMEM, then cultured in Endothelial Growth Media 2 (EGM-2;

Lonza, Walkersville, MD) with a final concentration of 50 ng/ml vascular endothelial growth factor ($VEGF_{165}$; Pierce Biotechnology, Rockford, IL). EGM-2 contained epidermal growth factor, hydrocortisone, GA-1000 (gentamicin, amphotericin-b), fetal bovine serum, basic fibroblast growth factor, insulin-like growth factor, ascorbic acid, and heparin at manufacturer concentrations. After 14 days, AFSC were stained with fluorescently-conjugated antibodies towards human CD31/PECAM (FITC IgG1κ, BD Biosciences; primary and isotype antibodies used at manufacturer recommended concentrations) and sorted to isolate the CD31-positive, endothelial-like population (AFSC-EC). FACSDiva software (BD Biosciences) was used for all flow cytometry data collection. FlowJo software (Tree Star, Inc., Ashland, OR) was used for data analysis.

2.3. Preparation of Fibrin/PEG Hydrogels Components

Fibrin/PEG-based hydrogels were prepared based on work previously described, [37, 40, 41] with slight variations. Human fibrinogen (F3879, Sigma-Aldrich, St Louis, MO) was solubilized in phosphate-buffered saline (PBS, 21-030-CV; Corning, Manassas, VA; adjusted to pH 7.8) at a concentration of 80 mg/mL. After 2 hours of incubation at 37°C, the solution was filtered using a 0.20 µm SteriFlip filter (EMD Millipore, Billerica, MA). Succinimidyl glutarate-modified bifunctional poly(ethylene glycol) (3.4 kDa SG-PEG-SG; NOF America Corporation, White Plains, NY) was dissolved in pH 7.8 PBS at 8 mg/ml and syringe filtered. Fibrinogen and PEG solutions were combined in a 1:1 volume ratio (10:1 PEG:fibrinogen MW ratio), mixed thoroughly, and incubated at 37°C for 6 hours. PEGylated fibrinogen was mixed at a 1:1 volume ratio with either pH 7.8 PBS (for no cell controls) or cell solution (200k cells/mL; co-cultures seeded at a 4:1 endothelial-to-stem cell ratio). Cell types and combinations encapsulated were

AFSC, AFSC-EC, AFSC/AFSC-EC, human mesenchymal stem cells (MSC), human umbilical vein endothelial cells (HUVEC), and MSC/HUVEC. All AFSC-derived cells were used at the same passage – undifferentiated AFSC were expanded for two weeks in the maintenance media described previously while the AFSC-EC subpopulation was differentiated and sorted. Human thrombin (T7009, Sigma-Aldrich) was diluted to 25U/mL in sterile 40 mM CaCl2 (208291; CalBiochem, La Jolla, CA) and incubated at 37°C prior to use.

2.4. Characterization of Fibrin/PEG Hydrogels Pre-Injection

2.4.1. Morphology

The microstructure of fibrin/PEG hydrogels was analyzed using scanning electron microscopy (Nova NanoSEM 230; FEI, Hillsboro, OR). Hydrogels were fixed in 4% paraformaldehyde (Alfa Aesar, Ward Hill, MA), dehydrated using serial dilution in ethanol (EX0276-3; Millipore), and dried using a critical point dryer (K850; EMI Tech Inc., Fall River, MA). Samples were sputter-coated (208HR; Cressington Scientific, Watford, England, UK) with a 5nm thick layer of platinum, and SEM images were taken between 5.0-7.0 keV and 5-15k magnification using xT Microscope Control software (FEI).

2.4.2. PEGylation Rate

To assess the effect of reaction time on the PEGylation of fibrinogen, 80 mg/mL fibrinogen was combined 1:1 with 8 mg/mL PEG and incubated at 37°C for various lengths of time (0, 1, 5, 20 minutes; 1, 6, 24 hours). At this point, the ester-amine reaction between PEG and fibrinogen was quenched using 50 mM tris[hydroxymethyl]aminomethane (Tris, 161-0716, Bio-Rad, Hercules, CA), and samples were denatured using β-marcaptoethanol (161-0710, Bio-

Rad) and boiling for 5 minutes. The samples were electrophoresed by 0.1% sodium dodecyl sulfate-polyacrylamide gel electrophoresis through 4-15% Mini-PROTEAN precast polyacrylamide gels (456-1083, Bio-Rad) at 100 V for 1.5 hours. Gels were stained with 0.125% Coomassie Brilliant Blue R-250 (20278, Thermo Scientific, Rockford, IL) in 40% methanol and 10% glacial acetic acid overnight, then destained for 24 hours in 20% methanol and 5% glacial acetic acid. Gels were rinsed with deionized water, and then scanned using a Gel Doc XR+ System (Bio-Rad) with automatic exposure adjustment.

2.5. Subcutaneous Injection of Fibrin/PEG Hydrogels

In vivo vascularization of fibrin/PEG hydrogels was assessed through subcutaneous implantation in aythymic nude mice in an experimental protocol approved by the Animal Care and Use Committees of Baylor College of Medicine and Rice University. Athymic nude mice (6-7 weeks old, Foxn1^{nu}, Harlan Laboratories, Indianapolis, IN) were chosen to minimize the immune response when encapsulating human-derived cells. Briefly, mice were anesthetized and injected in two dorsal, posterior subcutaneous areas on either side of midline with a combination of 125µl PEGylated fibrinogen, either 125µl sterile PBS or cell solution, and 250µl thrombin (all as previously described) at a ratio of 1:1:2, respectively, and a final concentration of 10mg/mL fibrinogen, 1mg/mL PEG, 5x10^4 cells, and 12.5U/mL thrombin. Cell types and combinations encapsulated were no cell control, AFSC, AFSC-EC, AFSC/AFSC-EC, MSC, HUVEC, and MSC/HUVEC. After 1 week, two additional subcutaneous injections were performed in each mouse so that when explanting the hydrogels at Day 14, both 1 and 2 week samples were obtained from the same animal.

2.6. Fibrin/PEG Hydrogel Analysis

2.6.1. Explanting and Sectioning Hydrogels

At day 14, mice were euthanized and fibrin/PEG hydrogels were explanted while retaining the underlying skin and connective tissue. Hydrogels were sectioned at the Baylor College of Medicine Breast Cancer Pathology core facility. Briefly, cells were fixed in 4% paraformaldehyde, serially dehydrated in ethanol, cleared with xylenes, and embedded in paraffin using the Sakura Tissue-Tek VIP Processor and Paraffin Embedding Center (Sakura FineTek USA Inc, Torrance, CA). The scaffolds were then sectioned using an HM 315 microtome (Richard-Allan Scientific / Thermo Scientific, Waltham, MA) at a thickness of 5μm.

2.6.2. Morphological Assessment

Hematoxylin and eosin staining of sectioned slides was done using a Shandon Varistain 24-4 Automatic Slide Stainer (Thermo Scientific). Slides were scanned at 2x using a OpticLab H850 slide scanner (PlusTek, UK), then imaged at 10x using an Eclipse E800 microscope and accompanying NIS-Elements software (Nikon Instruments Inc., Melville, NY). High-resolution photos of each hydrogel section (up to 40 per sample) were digitally merged using the Automate→Photomerge→Reposition feature in Photoshop (Adobe System, San Jose, CA), which allows for stitching images together automatically while retaining the original files' resolution and scale.

2.6.3. Analysis of Host Cell Invasion Rate

Merged high-resolution images of 1 and 2 week No Cell Control hydrogel sections were analyzed using MATLAB (MathWorks, Natick, MA) to assess the rate of host cell invasion in to the hydrogels. Image file names were blinded to the user, then an .m file was created to ask the

user to digitally outline the edge of hydrogel, ask the user to click on any number of cells (we selected 50+ cells furthest in to each sample), and then calculate the closest distance in μm from each cell to the hydrogel boundary and averages them.

2.6.4. Analysis of Lumen Formation

Similarly, merged high-resolution images of cell-seeded hydrogel sections were analyzed using MATLAB to assess the degree of lumen formation. Though many small areas of the hydrogel sections show degraded scaffold or cell structures in circular patterns, "lumen" was defined in this study as completely cell-lined, scaffold-free areas within the hydrogel. Image file names were blinded to the user, then an .m file was created to ask the user to digitally outline an area of the hydrogel to assess for vascularization, ask the user to click on any number of cells (we selected all lumenal structures in each given area), and then calculate the number of lumen per selected area in lumen/mm^2 and average them.

2.6.5. Immunostaining for Vascular Cell Types

To observe the organization of vascular cell types within the fibrin/PEG implants, slides were rehydrated, treated for antigen retrieval (heat-mediated, citrate-buffered retrieval; ab973, Abcam), permeabilized with Triton X100 (CalBioChem, San Diego, CA), and stained with αSMA (1:50; ab7817, Abcam, Cambridge, MA) and CD31 (1:50; ab28364, Abcam) overnight at 4°C. Secondary antibodies were used at 1:500 (Jackson ImmunoResearch Laboratories, Inc., West Grove, PA) for 30 minutes at room temperature. Cells were then counterstained with 4′,6-diamidino-2-phenylindole (DAPI) with Vecta Shield (Vector, Burlingame, CA). Images were

obtained using a DMI 6000B (Lieca Microsystems, Bannockburn, IL) fluorescence microscope and Leica Application Suite software.

2.7. Statistical Analysis

Data are expressed as mean ± standard deviation. Analysis of variance flowed by a post-hoc Student's t-test with a Dunn-Bonferroni correction for multiple comparisons was performed for all comparisons. A value of $p<0.05$ was considered significant in all tests.

3. RESULTS

Characterization of Fibrin/PEG Hydrogels

SEM images display thin fibril structures within fibrin-only hydrogels and larger bundled structures within fibrin/PEG hydrogels. (Fig 1A) Pores throughout individual samples were not uniform in size, but porosity in fibrin-only hydrogels was significantly greater than fibrin/PEG hydrogels (81.7%±6.51% vs 70.7%±8.17, respectively). (Fig 1B)

Fibrinogen samples were PEGylated at a 10:1 molar ratio of PEG:fibrinogen at time points ranging from 1 minute to 24 hours. (Fig 1C) Quantification of gel electrophoresis data was done using the *Gel Analysis* feature within ImageJ. (Fig 1D) The percentage of total protein per band was calculated as fractions of fibrinogen (40-70 kDa range), low-molecular weight PEGylated fibrinogen (70-250kDa), and high-molecular weight PEGylated fibrinogen (250+ kDa), all normalized to fibrinogen-only samples. For PEGylation times of 1min, 5min, 20min, 1hr, 3hr, 6hr, and 24hr, fractions of fibrinogen-only were (63.7%, 53.7%, 47.4%, 46.0%, 43.6%, 43.8%, 43.4%, respectively), fractions of low-MW PEGylated fibrinogen were (34.5%, 37.2%, 40.4%, 40.4%, 39.0%, 41.8%, 41.6%, respectively), and fractions of high-MW PEGylated fibrinogen were (1.9%, 9.1%, 12.2%, 13.6%, 17.5%, 14.4%, 15.0%, respectively).

Subcutaneous Injection of Fibrin/PEG Hydrogels

Hydrogels subcutaneously injected on the dorsal side of an athymic nude mouse were clearly intact two weeks post-implantation. (Fig 2A/B) Explanted control hydrogels without cell-seeding were explanted at 1 and 2 weeks post-injection then fixed, paraffin sectioned, and stained with hematoxylin and eosin. Host cell invasion can clearly been seen in high-resolution images. (Fig 2D) Based on these controls, the average maximum distance of host cell infiltration in to the subcutaneous fibrin/PEG scaffold was calculated to be 147.2±90.1μm after one week and 394.8±137.7μm after two weeks. (Fig 2C)

Cell-seeded hydrogels were explanted at 2 weeks post-injection, then fixed, sectioned, and H&E stained. (Fig 3A-D) Slides scanned at 2x showed qualitative differences between samples, such as the large vascular structures seen in (Fig 3D), while imaged taken at 10x revealed smaller erythrocyte-filled lumen in other samples (Fig 3A).

Assessment of Hydrogel Vascularization

The degree of lumen formation was determined by comparing the number of cell-lined vessels per mm^2 in sections of various cell-seeded hydrogels. The average density of cell-lined vessels (in lumen per mm^2) was significantly higher in hydrogels seeded with stem cells or co-cultures containing stem cells (MSC, 36.5±11.4; AFSC, 47.0±18.9; AFSC/AFSC-EC, 32.8±11.6; MSC/HUVEC, 43.1±25.1 lumen per mm^2) versus endothelial cell types alone (AFSC-EC, 9.7±6.1; HUVEC, 14.2±8.8 lumen per mm^2) or hydrogels without cells (0.21±0.06 lumen per mm^2). A subset of these lumen were characterized by the presence of red blood cells, but there was no significant difference between groups (without cells, 0.02±0.02; AFSC-EC, 1.82±1.63; HUVEC, 1.94±0.99; MSC, 10.68±10.13; AFSC, 8.27±6.44; AFSC/AFSC-EC, 5.59±4.35; MSC/HUVEC, 8.55±7.77 lumen per mm^2). (Fig 3C/D)

Sections of hydrogel explanted at two weeks were stained for the presence of smooth muscle cells (αSMA) and endothelial cells (CD31), then counterstained with DAPI. No cell controls showed αSMA-positive host cells infiltrating the fibrin/PEG scaffold, (Fig 4A) while AFSC/AFSC-EC and MSC/HUVEC seeded hydrogels showed a cleared interaction between CD31-positive and αSMA-positive cells. Select areas of cell-seeded hydrogels contained dual-positive CD31/α-SMA lumen, whereas no cell control did not. (Fig 4B/C)

4. DISCUSSION

The first use of amniotic fluid as a diagnostic tool for genetic abnormalities was in 1956, yet only recently has it been explored for stem and progenitor cell populations.[24, 42, 43] AFSC have since been shown to be a significant source of vascular cell types and have the potential for use in regenerative medicine strategies, such as engineered skeletal/cardiac muscle, tendons, heart valves, and blood vessels.[24, 43-46]

This study expands on our previous work assessing the in vitro vasculogenic potential of AFSC within a three-dimensional fibrin/PEG scaffold.[25] A subcutaneous model was chosen for in vivo evaluation in order to facilitate in situ polymerization of fibrin-based hydrogels and minimize the trauma associated with alternative methods of vascular assessment, such as those that create a pocket between the fascia and muscle.[47] With this model, other groups have demonstrated very low background wound-healing and inflammatory responses, which allows for evaluation of the inductive effects of the exogenous engineered tissue rather than the chemotactic effect of angiogenic cytokines, such as those in blood, which could perfuse implanted hydrogels in a surgical approach. [48]

Because various groups have used a fibrinogen PEGylation reaction time ranging from minutes to hours,[41, 49-51] the optimal reaction time was assessed prior to in vivo use. The high-molecular weight of native fibrinogen (340 kDa), combined with the PEG-driven crosslinking, makes assessing the rate of PEGylation difficult. By denaturing fibrinogen into fibrinopeptide subunits (45-65 kDa),[52] the reaction can be tracked using standard polyacrylamide gel electrophoresis. Our results suggest that the PEGylation of fibrinogen was maximized after approximately one hour. The maximum percentage of fibrinogen modified by PEG at this point is comparable to other reported values,[49] and the driving factor is hypothesized to be the hydrolysis half life of the reactive ester group on this PEG variant, which ranges from 10 minutes to 4 hours.[38, 53]

Control hydrogels without cells injected in this murine model showed host cell infiltration on the order of 20-25 μm/day, which is in agreement with reported values of PEG/fibrin hydrogels with similar fibrinogen concentrations.[48] A subpopulation of invading cells stained positive for αSMA, suggesting proliferation and migration of fibroblasts from the underlying fascia layer.

When analyzing the degree of lumen formation within cell-seeded hydrogel sections, as well as the presence of red blood cells, a large degree of variability was seen. A number of factors could play an important role in these results, including injection placement, underlying vascular networks, and inherent animal variability. One significant result was that hydrogels containing MSCs or AFSCs either alone or in co-cultures produced significantly more lumen formation compared to endothelial cell-types alone. Based on our *in vitro* data in similar hydrogels,[25] we had hypothesized that the development of robust vasculature would require the presence of both exogenous endothelial and perivascular cell sources; however, in similar

subcutaneous mouse studies, vascularization was not significantly different between fibrin-based constructs seeded with MSC/HUVEC co-cultures compared to those seeded with MSC only.[18]

Recent insight in to the secretome of AFSCs may help explain these results. Paracrine factors produced by AFSCs, including vascular endothelial growth factor, stromal cell-derived factor 1, interleukin 8, and monocyte chemotactic protein 1, were isolated and shown to be capable of enhancing vasculogenesis in a murine model.[54] This combination of pro-angiogenic cytokines has a clear effect on the recruitment of endothelial cell types specifically[55] and could mask the effects seen by introducing exogenous vascular cells.[56]

In this study, *in situ* vascularization of subcutaneously injected fibrin/PEG hydrogels was clearly correlated to the presence of a stem cell source, either AFSC or MSC; however, in order to understand the role that AFSC and AFSC-EC play in *in vivo* vessel formation, further analysis is required. Determining the localization of exogenous cells in both the bulk of the hydrogel and in relation to the formation of dual-positive CD31/αSMA lumen will be critical to assessing the therapeutic potential of AFSC-derived vascularization.

5. ACKNOWLEDGMENTS

We thank Texas Children Hospital's Maternal-Fetal Medicine Center for supplying the amniotic fluid, Dr. Joel Moake for generously providing the HUVEC, Dr. Vivek Kumar for guidance with animal models and immunohistochemisty, and the Baylor College of Medicine Breast Cancer Pathology Lab for their histology expertise.

6. GRANTS

This study was supported by the supported by the NIH (OMB), NSF GRFP (JPC), and NSF CAREER (JGJ).

7. DISCLOSURES

There are no competing financial interests.

8. REFERENCES

[1] Levenberg S, Rouwkema J, Macdonald M, Garfein ES, Kohane DS, Darland DC, et al. Engineering vascularized skeletal muscle tissue. Nature biotechnology. 2005;23:879-84.
[2] Langer R, Vacanti JP. Tissue engineering. Science. 1993;260:920-6.
[3] Jain RK, Au P, Tam J, Duda DG, Fukumura D. Engineering vascularized tissue. Nature biotechnology. 2005;23:821-3.
[4] Colton CK. Implantable biohybrid artificial organs. Cell transplantation. 1995;4:415-36.
[5] Folkman J, Hochberg M. Self-regulation of growth in three dimensions. The Journal of experimental medicine. 1973;138:745-53.
[6] Muschler GF, Nakamoto C, Griffith LG. Engineering principles of clinical cell-based tissue engineering. The Journal of bone and joint surgery American volume. 2004;86-A:1541-58.
[7] Isner JM, Asahara T. Angiogenesis and vasculogenesis as therapeutic strategies for postnatal neovascularization. The Journal of clinical investigation. 1999;103:1231-6.
[8] Lee H, Cusick RA, Browne F, Ho Kim T, Ma PX, Utsunomiya H, et al. Local delivery of basic fibroblast growth factor increases both angiogenesis and engraftment of hepatocytes in tissue-engineered polymer devices. Transplantation. 2002;73:1589-93.
[9] Nillesen ST, Geutjes PJ, Wismans R, Schalkwijk J, Daamen WF, van Kuppevelt TH. Increased angiogenesis in acellular scaffolds by combined release of FGF2 and VEGF. Journal of controlled release : official journal of the Controlled Release Society. 2006;116:e88-90.
[10] Laschke MW, Vollmar B, Menger MD. Inosculation: connecting the life-sustaining pipelines. Tissue engineering Part B, Reviews. 2009;15:455-65.
[11] Frerich B, Lindemann N, Kurtz-Hoffmann J, Oertel K. In vitro model of a vascular stroma for the engineering of vascularized tissues. International journal of oral and maxillofacial surgery. 2001;30:414-20.
[12] Rivron NC, Liu JJ, Rouwkema J, de Boer J, van Blitterswijk CA. Engineering vascularised tissues in vitro. European cells & materials. 2008;15:27-40.
[13] Zarem HA. The microcirculatory events within full-thickness skin allografts (homografts) in mice. Surgery. 1969;66:392-7.
[14] Orr AW, Elzie CA, Kucik DF, Murphy-Ullrich JE. Thrombospondin signaling through the calreticulin/LDL receptor-related protein co-complex stimulates random and directed cell migration. Journal of cell science. 2003;116:2917-27.

[15] Fontaine M, Schloo B, Jenkins R, Uyama S, Hansen L, Vacanti JP. Human hepatocyte isolation and transplantation into an athymic rat, using prevascularized cell polymer constructs. Journal of pediatric surgery. 1995;30:56-60.
[16] Chen X, Aledia AS, Ghajar CM, Griffith CK, Putnam AJ, Hughes CC, et al. Prevascularization of a fibrin-based tissue construct accelerates the formation of functional anastomosis with host vasculature. Tissue engineering Part A. 2009;15:1363-71.
[17] Caspi O, Lesman A, Basevitch Y, Gepstein A, Arbel G, Habib IH, et al. Tissue engineering of vascularized cardiac muscle from human embryonic stem cells. Circulation research. 2007;100:263-72.
[18] Verseijden F, Posthumus-van Sluijs SJ, van Neck JW, Hofer SO, Hovius SE, van Osch GJ. Vascularization of prevascularized and non-prevascularized fibrin-based human adipose tissue constructs after implantation in nude mice. Journal of tissue engineering and regenerative medicine. 2012;6:169-78.
[19] Melero-Martin JM, De Obaldia ME, Kang SY, Khan ZA, Yuan L, Oettgen P, et al. Engineering robust and functional vascular networks in vivo with human adult and cord blood-derived progenitor cells. Circulation research. 2008;103:194-202.
[20] Melero-Martin JM, Khan ZA, Picard A, Wu X, Paruchuri S, Bischoff J. In vivo vasculogenic potential of human blood-derived endothelial progenitor cells. Blood. 2007;109:4761-8.
[21] Kreutziger KL, Muskheli V, Johnson P, Braun K, Wight TN, Murry CE. Developing vasculature and stroma in engineered human myocardium. Tissue engineering Part A. 2011;17:1219-28.
[22] Benavides OM, Petsche JJ, Moise KJ, Jr., Johnson A, Jacot JG. Evaluation of endothelial cells differentiated from amniotic fluid-derived stem cells. Tissue engineering Part A. 2012;18:1123-31.
[23] Petsche Connell J, Camci-Unal G, Khademhosseini A, Jacot JG. Amniotic fluid-derived stem cells for cardiovascular tissue engineering applications. Tissue engineering Part B, Reviews. 2013;19:368-79.
[24] De Coppi P, Bartsch G, Jr., Siddiqui MM, Xu T, Santos CC, Perin L, et al. Isolation of amniotic stem cell lines with potential for therapy. Nature biotechnology. 2007;25:100-6.
[25] Benavides OM, Quinn JP, Pok S, Connell JP, Ruano R, Jacot JG. Capillary-like Network Formation by Human Amniotic Fluid-Derived Stem Cells within Fibrin/Poly(Ethylene Glycol) Hydrogels (in submission). 2014.
[26] Pok S, Benavides OM, Hallal P, Jacot JG. Use of myocardial matrix in a chitosan-based full-thickness heart patch. Tissue engineering Part A. 2014;20:1877-87.
[27] Pok S, Jacot JG. Biomaterials advances in patches for congenital heart defect repair. Journal of cardiovascular translational research. 2011;4:646-54.
[28] Shastri VP. In vivo engineering of tissues: Biological considerations, challenges, strategies, and future directions. Adv Mater. 2009;21:3246-54.
[29] Jockenhoevel S, Zund G, Hoerstrup SP, Chalabi K, Sachweh JS, Demircan L, et al. Fibrin gel -- advantages of a new scaffold in cardiovascular tissue engineering. European journal of cardio-thoracic surgery : official journal of the European Association for Cardio-thoracic Surgery. 2001;19:424-30.
[30] Zhang G, Suggs LJ. Matrices and scaffolds for drug delivery in vascular tissue engineering. Advanced drug delivery reviews. 2007;59:360-73.
[31] van Hinsbergh VW, Collen A, Koolwijk P. Role of fibrin matrix in angiogenesis. Annals of the New York Academy of Sciences. 2001;936:426-37.

[32] Wittmann K, Storck K, Muhr C, Mayer H, Regn S, Staudenmaier R, et al. Development of volume-stable adipose tissue constructs using polycaprolactone-based polyurethane scaffolds and fibrin hydrogels. Journal of tissue engineering and regenerative medicine. 2013.
[33] Klar AS, Guven S, Biedermann T, Luginbuhl J, Bottcher-Haberzeth S, Meuli-Simmen C, et al. Tissue-engineered dermo-epidermal skin grafts prevascularized with adipose-derived cells. Biomaterials. 2014;35:5065-78.
[34] Atluri P, Miller JS, Emery RJ, Hung G, Trubelja A, Cohen JE, et al. Tissue-engineered, hydrogel-based endothelial progenitor cell therapy robustly revascularizes ischemic myocardium and preserves ventricular function. The Journal of thoracic and cardiovascular surgery. 2014;148:1090-8.
[35] Kannan RY, Salacinski HJ, Sales K, Butler P, Seifalian AM. The roles of tissue engineering and vascularisation in the development of micro-vascular networks: a review. Biomaterials. 2005;26:1857-75.
[36] Shaikh FM, Callanan A, Kavanagh EG, Burke PE, Grace PA, McGloughlin TM. Fibrin: a natural biodegradable scaffold in vascular tissue engineering. Cells, tissues, organs. 2008;188:333-46.
[37] Zhang G, Wang X, Wang Z, Zhang J, Suggs L. A PEGylated fibrin patch for mesenchymal stem cell delivery. Tissue engineering. 2006;12:9-19.
[38] Natesan S, Zhang G, Baer DG, Walters TJ, Christy RJ, Suggs LJ. A bilayer construct controls adipose-derived stem cell differentiation into endothelial cells and pericytes without growth factor stimulation. Tissue engineering Part A. 2011;17:941-53.
[39] Connell JP, Augustini E, Moise KJ, Jr., Johnson A, Jacot JG. Formation of functional gap junctions in amniotic fluid-derived stem cells induced by transmembrane co-culture with neonatal rat cardiomyocytes. Journal of cellular and molecular medicine. 2013;17:774-81.
[40] Zhang G, Hu Q, Braunlin EA, Suggs LJ, Zhang J. Enhancing efficacy of stem cell transplantation to the heart with a PEGylated fibrin biomatrix. Tissue engineering Part A. 2008;14:1025-36.
[41] Seetharaman S, Natesan S, Stowers RS, Mullens C, Baer DG, Suggs LJ, et al. A PEGylated fibrin-based wound dressing with antimicrobial and angiogenic activity. Acta biomaterialia. 2011;7:2787-96.
[42] Fuchs F, Riis P. Antenatal sex determination. Nature. 1956;18.
[43] Delo DM, De Coppi P, Bartsch G, Jr., Atala A. Amniotic fluid and placental stem cells. Methods in enzymology. 2006;419:426-38.
[44] In 't Anker PS, Scherjon SA, Kleijburg-van der Keur C, Noort WA, Claas FH, Willemze R, et al. Amniotic fluid as a novel source of mesenchymal stem cells for therapeutic transplantation. Blood. 2003;102:1548-9.
[45] Bollini S, Pozzobon M, Nobles M, Riegler J, Dong X, Piccoli M, et al. In vitro and in vivo cardiomyogenic differentiation of amniotic fluid stem cells. Stem cell reviews. 2011;7:364-80.
[46] Decembrini S, Cananzi M, Gualdoni S, Battersby A, Allen N, Pearson RA, et al. Comparative analysis of the retinal potential of embryonic stem cells and amniotic fluid-derived stem cells. Stem cells and development. 2011;20:851-63.
[47] Chiu YC, Larson JC, Isom A, Jr., Brey EM. Generation of porous poly(ethylene glycol) hydrogels by salt leaching. Tissue engineering Part C, Methods. 2010;16:905-12.
[48] Jiang B, Waller TM, Larson JC, Appel AA, Brey EM. Fibrin-loaded porous poly(ethylene glycol) hydrogels as scaffold materials for vascularized tissue formation. Tissue engineering Part A. 2013;19:224-34.

[49] Xu H, Kaar JL, Russell AJ, Wagner WR. Characterizing the modification of surface proteins with poly(ethylene glycol) to interrupt platelet adhesion. Biomaterials. 2006;27:3125-35.
[50] Zamora DO, Natesan S, Becerra S, Wrice N, Chung E, Suggs LJ, et al. Enhanced wound vascularization using a dsASCs seeded FPEG scaffold. Angiogenesis. 2013;16:745-57.
[51] Galler KM, Cavender AC, Koeklue U, Suggs LJ, Schmalz G, D'Souza RN. Bioengineering of dental stem cells in a PEGylated fibrin gel. Regenerative medicine. 2011;6:191-200.
[52] Henschen A, Lottspeich F, Kehl M, Southan C. Covalent structure of fibrinogen. Annals of the New York Academy of Sciences. 1983;408:28-43.
[53] Hayworth D. Amine-reactive Crosslinker Chemistry. 2008.
[54] Mirabella T, Cilli M, Carlone S, Cancedda R, Gentili C. Amniotic liquid derived stem cells as reservoir of secreted angiogenic factors capable of stimulating neo-arteriogenesis in an ischemic model. Biomaterials. 2011;32:3689-99.
[55] Mirabella T, Hartinger J, Lorandi C, Gentili C, van Griensven M, Cancedda R. Proangiogenic soluble factors from amniotic fluid stem cells mediate the recruitment of endothelial progenitors in a model of ischemic fasciocutaneous flap. Stem cells and development. 2012;21:2179-88.
[56] Roubelakis MG, Trohatou O, Anagnou NP. Amniotic fluid and amniotic membrane stem cells: marker discovery. Stem cells international. 2012;2012:107836.

9. FIGURE LEGENDS

Figure 1 – Characterization of Fibrin/PEG Hydrogels. (A) SEM images display thin fibril structures within fibrin-only hydrogels and larger bundled structures within fibrin/PEG hydrogels. Scale bars are 10μm. (B) Pores throughout individual samples were not uniform in size, but porosity in fibrin-only hydrogels was significantly greater ($p<0.05$) than fibrin/PEG hydrogels. (C) Fibrinogen samples were PEGylated at a 10:1 molar ratio of PEG:fibrinogen at time points ranging from 1 minute to 24 hours. (D) Quantification of Western blot data was done using ImageJ. The percentage of total protein per band was calculated as fractions of fibrinogen (40-70 kDa range), low-molecular weight PEGylated fibrinogen (70-250kDa), and high-molecular weight PEGylated fibrinogen (250+ kDa).

Figure 2 – Subcutaneous injection of fibrin/PEG hydrogels. (A) Hydrogel implant on the back of an athymic nude mouse ($Foxn1^{nu}$). Scale bar is 2cm. (B) Explanted no cell control and AFSC/AFSC-EC co-culture hydrogels at 2 week post-injection. Scale bars are 5mm. Explants were fixed and paraffin sectioned, then stained with hematoxylin and eosin to assess general morphology. Samples were scanned at 2x (shown), as well as imaged at 10x and digitally

merged for analysis. Representative images of (C) AFSC-only, (D) AFSC-EC-only, (E) AFSC/AFSC-EC, and (F) MSC/HUVEC-seeded hydrogels explanted at 2 weeks then H&E stained. Scale bars are 500µm for slide scans and 100µm for magnified images.

Figure 3 – Quantitative analysis of hydrogel vascularization. (A) At 1 and 2 weeks, sections of no-cell control hydrogels were stained with hematoxylin and eosin. Scale bars are 500µm for slide scans and 100µm for magnified images. (B) Based on these controls, the rate of host cell invasion was assessed. (C) The degree of lumen formation was determined by comparing the number of cell-lined vessels per mm^2 in sections of various cell-seeded hydrogels (AFSC, AFSC-EC, MSC, HVUEC, AFSC/AFSC-EC, and MSC/HUVEC). Bars which share a letter were not significantly different from each other. A value of $p<0.05$ was considered significant. A subset of this group was characterized by the presence of red blood cells; however, there was no significant deference between groups tested. Representative images of both (D) AFSC/AFSC-EC and (E) MSC/HUVEC co-cultures are shown. Scale bars are100µm.

Figure 4 – Assessment of vascular morphology. At 2 weeks, explanted hydrogels were stained for the presence of smooth muscle cells (α-smooth muscle actin; green) and endothelial cells (CD31; red), then counterstained with DAPI (blue). (A) No cell controls, (B) AFSC/AFSC-EC seeded hydrogels, and (C) MSC/HUVEC seeded hydogels shown here. Scale bars are 50µm.

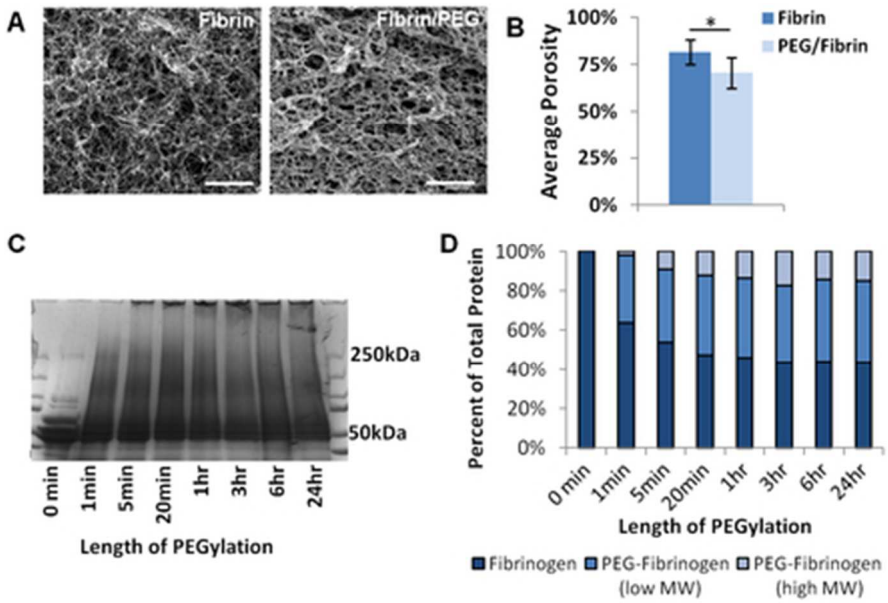

Figure 1 – Characterization of Fibrin/PEG Hydrogels. (A) SEM images display thin fibril structures within fibrin-only hydrogels and larger bundled structures within fibrin/PEG hydrogels. Scale bars are 10μm. (B) Pores throughout individual samples were not uniform in size, but porosity in fibrin-only hydrogels was significantly greater ($p<0.05$) than fibrin/PEG hydrogels. (C) Fibrinogen samples were PEGylated at a 10:1 molar ratio of PEG:fibrinogen at time points ranging from 1 minute to 24 hours. (D) Quantification of Western blot data was done using ImageJ. The percentage of total protein per band was calculated as fractions of fibrinogen (40-70 kDa range), low-molecular weight PEGylated fibrinogen (70-250kDa), and high-molecular weight PEGylated fibrinogen (250+ kDa).
37x25mm (300 x 300 DPI)

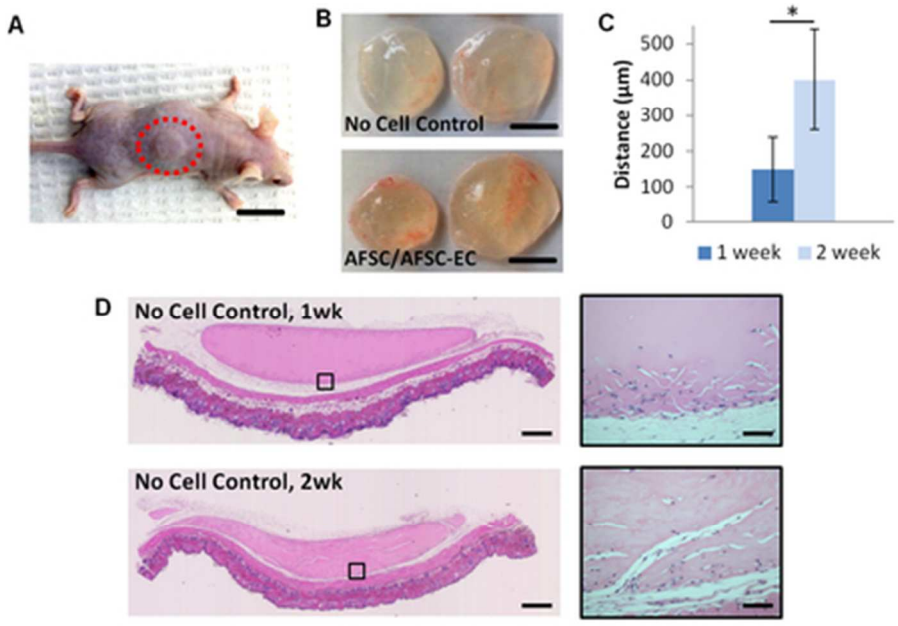

Figure 2 – Subcutaneous injection of fibrin/PEG hydrogels. (A) Hydrogel implant on the back of an athymic nude mouse (Foxn1nu). Scale bar is 2cm. (B) Explanted no cell control and AFSC/AFSC-EC co-culture hydrogels at 2 week post-injection. Scale bars are 5mm. Explants were fixed and paraffin sectioned, then stained with hematoxylin and eosin to assess general morphology. Samples were scanned at 2x (shown), as well as imaged at 10x and digitally merged for analysis. Representative images of (C) AFSC-only, (D) AFSC-EC-only, (E) AFSC/AFSC-EC, and (F) MSC/HUVEC-seeded hydrogels explanted at 2 weeks then H&E stained. Scale bars are 500μm for slide scans and 100μm for magnified images.
37x26mm (300 x 300 DPI)

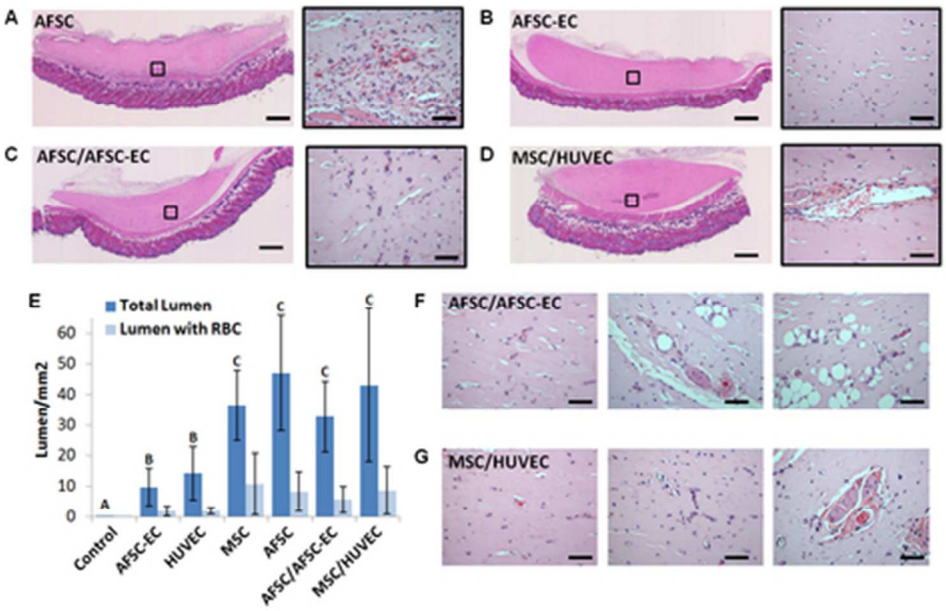

Figure 3 – Quantitative analysis of hydrogel vascularization. (A) At 1 and 2 weeks, sections of no-cell control hydrogels were stained with hematoxylin and eosin. Scale bars are 500μm for slide scans and 100μm for magnified images. (B) Based on these controls, the rate of host cell invasion was assessed. (C) The degree of lumen formation was determined by comparing the number of cell-lined vessels per mm2 in sections of various cell-seeded hydrogels (AFSC, AFSC-EC, MSC, HVUEC, AFSC/AFSC-EC, and MSC/HUVEC). Bars which share a letter were not significantly different from each other. A value of $p<0.05$ was considered significant. A subset of this group was characterized by the presence of red blood cells; however, there was no significant deference between groups tested. Representative images of both (D) AFSC/AFSC-EC and (E) MSC/HUVEC co-cultures are shown. Scale bars are100μm.
39x25mm (300 x 300 DPI)

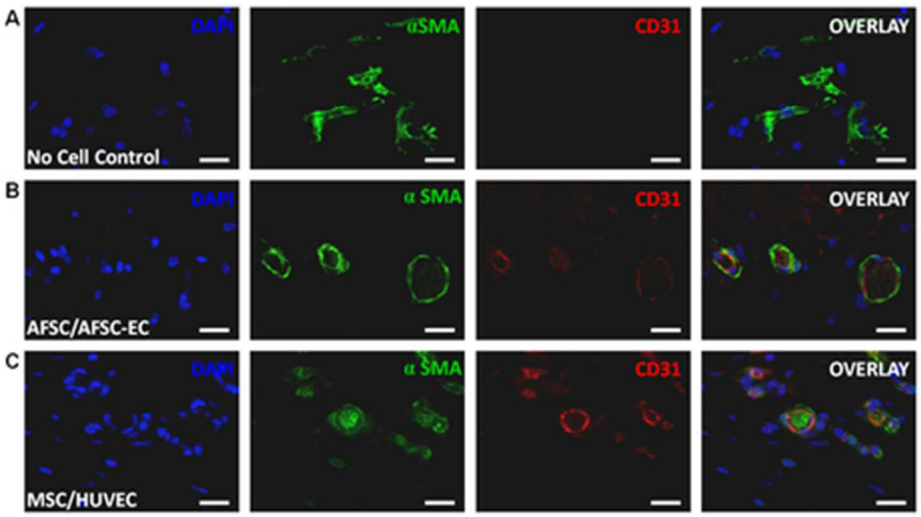

Figure 4 – Assessment of vascular morphology. At 2 weeks, explanted hydrogels were stained for the presence of smooth muscle cells (α-smooth muscle actin; green) and endothelial cells (CD31; red), then counterstained with DAPI (blue). (A) No cell controls, (B) AFSC/AFSC-EC seeded hydrogels, and (C) MSC/HUVEC seeded hydogels shown here. Scale bars are 50μm.
38x21mm (300 x 300 DPI)